ANNALI DI GEOFISICA, VOL. XXXIX, N. 1, January 1996

Inverse problem for tripotential measures in the study of buried cavities

Pietro Cosentino([1]), **Dario Luzio**([1]) **and Raffaele Martorana**([2])
([1]) *Istituto di Geofisica Mineraria, Università di Palermo, Italy*
([2]) *Geotop, Palermo, Italy*

Abstract
This paper presents a solution to the inverse electrical problem for the interpretation of apparent resistivity anomalies due to empty buried cavities of quasi-spherical shape when tripotential measures are carried out. The anomalies of the apparent resistivities ρ_α, ρ_β and ρ_γ, and the composed resistivities ρ_μ and ρ_τ were previously calculated for a sufficient class of spherical models of resistivity anomalies. Then, for the whole class of models, some functionals of spatial distribution of the apparent and composed resistivity were identified and analyzed. They represent the average characteristics of the anomalies and, depending in a simple way on the fundamental parameters of the sources of the anomalies (average diameter and depth), they allow reliable estimates to be determined. Among the studied functionals, those allowing the most stable and less biased estimates of the anomaly source parameters are identified by numerical simulations with random noise perturbed data. Finally the trend of standard deviation and bias of the estimates of the unknown parameters were analyzed by varying the source models and the set of functionals used for the inversion.

Key words *geoelectrical surveys – tripotential method – inverse problem – synthetic tests – cavities*

1. Introduction

To identify and characterize empty buried cavities the direct current geoelectrical methods are among the most effective techniques of geophysical investigation.

A survey methodology aimed at the study of cavities must provide for the acquisition of many experimental data superficially distributed and characterized by various depths of investigation. The most ordinary interpretation techniques are based on the solution of the direct problem, using the finite differences, or the finite elements or the boundary element methods. These techniques, which are the most suitable for very complex models, hardly apply to this problem because of the instabilities in the solution of the inverse problem caused by the complexity of the experimental signal, almost always characterized by a rather high geological noise, and the need to use models involving a very high number of unknowns, that cannot be adequately assessed.

In the case of quasi-spherical cavities, distinguishable by only three position parameters and one average extension parameter, an acquisition technique of experimental data rich in information is the Wenner type tripotential method. It will be shown that the latter allows a reliable solution to the inverse problem for the average parameters of the cavity by using a technique based on the calculus of some functionals of the experimental data of the type $F_i = F_i\,(d_j\,(j = 1, n);\, a/L,\, h/L)$, with d_j generic experimental datum, a radius of the cavity spherical model, h its minimum depth and L electrode spacing. Among such functionals we identified many of them characterized by generally strong biunivocal dependencies on one of the unknown parameters a/L or h/L once the value of the second is fixed (only for a few

functionals, in limited regions of the space of the parameters, two values of an unknown parameter correspond to one value of the functional and to one of the other unknown parameters). These conditions, and the phenomenological knowledge of functionals' dependencies on unknown parameters, generally allow the use of the estimates of any pair of such functionals in order to obtain univocal estimates of the parameters of the model. Through synthetic inversion tests based on the use of «experimental» data obtained by perturbing the direct problem solutions by an appropriate width random signal, we studied how the reliability of the estimates on the unknown parameters varies when these latter change.

2. Direct problem for spherical resistivity anomalies

According to Large's approach (1971) a code was been devised to calculate the electric potential due to a point source of electric current placed on the surface in proximity of a spherical buried body characterized by any resistivity.

With reference to a system of bispherical coordinates (T, σ, φ) for which it is simple to impose the boundary conditions on the ground and cavity surfaces (fig. 1), the solution to the equation for the potential, for a point of the conductive half space external to the sphere, can be expressed as

$$V = \frac{I_\rho}{2\pi}\left\{\frac{1}{R} + \frac{(1-\cos T_0)^{1/2}\,(\cos h\,\sigma - \cos T)^{1/2}}{b}\cdot \sum_{n=0}^{\infty}\sum_{m=0}^{n} a_{mn}\,(A_{mn}e^{N\sigma} + B_{mn}e^{-N\sigma})\cdot P_n^m(\cos T)\,P_n^m(\cos T_0)\cos(m\phi)\right\}, \qquad (2.1)$$

where m and n are integers, P_n^m are the associ-

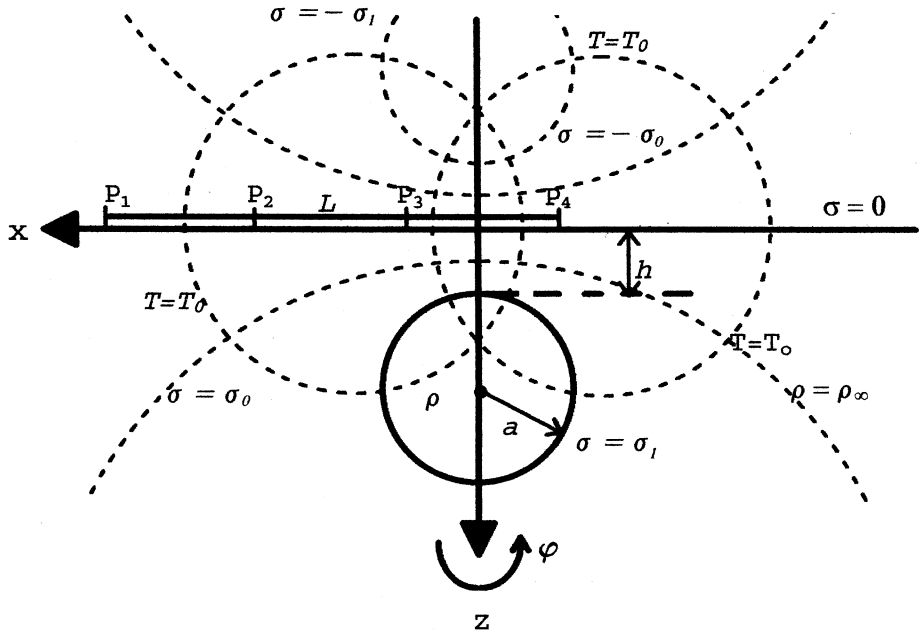

Fig. 1. Scheme of bispherical coordinates and of the type of array used: $\sigma = \sigma_1$ cavity surface, $\sigma = 0$ ground surface.

ated Legendre functions of the first type, of n degree and m order, and A_{mn} and B_{mn} are coefficients depending on the source position and on the geometric parameters of the model, obtained by imposing the asymptotic boundary conditions and the boundary conditions on the discontinuity surfaces. By (2.1), truncated to the degree $n = 12$ to allow the exact determination of at least five significant digits of the potential value, the calculus of the apparent resistivity anomalies was carried out. The anomalies caused by more than one hundred models of cavities of radius a between $0.1L$ and $4L$ and of minimum depth h between $0.1L$ and $2L$ were calculated in all the knots of a square mesh superficial grid with step $0.02L$, centered on the vertical of the cavity center. The measures are simulated in each point for two directions normal to one another, and in order to obtain anomalies not particularly dependent on the azimuth of the test point with reference to the superficial projection of the center of the sphere, we calculated the arithmetic averages $\langle \rho_i \rangle$, measured along the two directions.

Some anomaly maps of the ratios $\frac{\langle \rho_\alpha \rangle}{\rho_\infty}$, $\frac{\langle \rho_\beta \rangle}{\rho_\infty}$, $\frac{\langle \rho_\gamma \rangle}{\rho_\infty}$, and $\frac{\langle \rho_\mu \rangle}{\rho_\infty}$, where ρ_∞ is the mean resistivity of the medium containing the cavity, are shown in fig. 2.

A portion of model space which includes parameter values of potentially detectable cavities (in absence of noise) was initially located in the (a/L, h/L) space, considering that an anomaly is detectable if its amplitude is almost 10% of the value of the background resistivity in four test points, and considering also detectable those anomalies characterized by amplitudes whose values decrease to a minimum of 3% as the anomaly area increases. A maximum depth of investigation was then determined, for each ratio a/L, in terms of the ratio h/L. This analysis showed that, when the electrode spacing is larger than double the cavity mean radius or shorter than half of its minimum depth, the anomaly is unlikely to be detectable for any ratio h/a. For electrode spacing larger than $2h/3$ and shorter than $2a$ the maximum depth of investigation can be expressed by $h_{MAX} \leq 1.1a$.

In practice, the zone characterized by detectable models in parameters space must certainly be contained in the zone so defined; its extension will depend on the signal to noise ratio and could be expressed in terms of the relative variances and biases of the estimates of the unknown parameters. The estimates of these variances and biases, for a wide class of models, are here obtained assuming that random noise is uniformly distributed in the interval [0.9 ρ_∞, 1.1 ρ_∞].

3. Inverse problem

To evaluate the position and the mean radius of the sphere, which best describes the surface of the investigated cavity, it is possible to use a «phenomenological» approach based on the empirical research of those functionals of the experimental data which present a simple dependence correlation to the parameters of the models.

The coordinates of the projection of the center of the spherical model on the surface can be approximated to the coordinates of the average point of the anomaly of the composed resistivity ρ_μ (Cosentino *et al.*, 1992; Cosentino and Luzio, 1994). In order to determine the depth and the mean radius of the cavity, some parameters, that describe some average aspects of the anomalous field, were individuated. Their values were determined on eighty-one cavity models with a/L values between 0.1 and 4.1 (step 0.5) and with h/L values between 0.1 and 2.1 (step 0.25).

The following sections describe the most effective *inversion parameters* so far analyzed for data interpretation.

3.1. *Area of the apparent resistivity anomaly*

The extension Δ_i of the area which includes an anomaly in the apparent resistivity caused by a cavity, is a characteristic of the anomalous field depending both on the depth of the sphere's top and on its radius. It can therefore be useful to consider this quantity as an additional parameter useful to solve the inverse

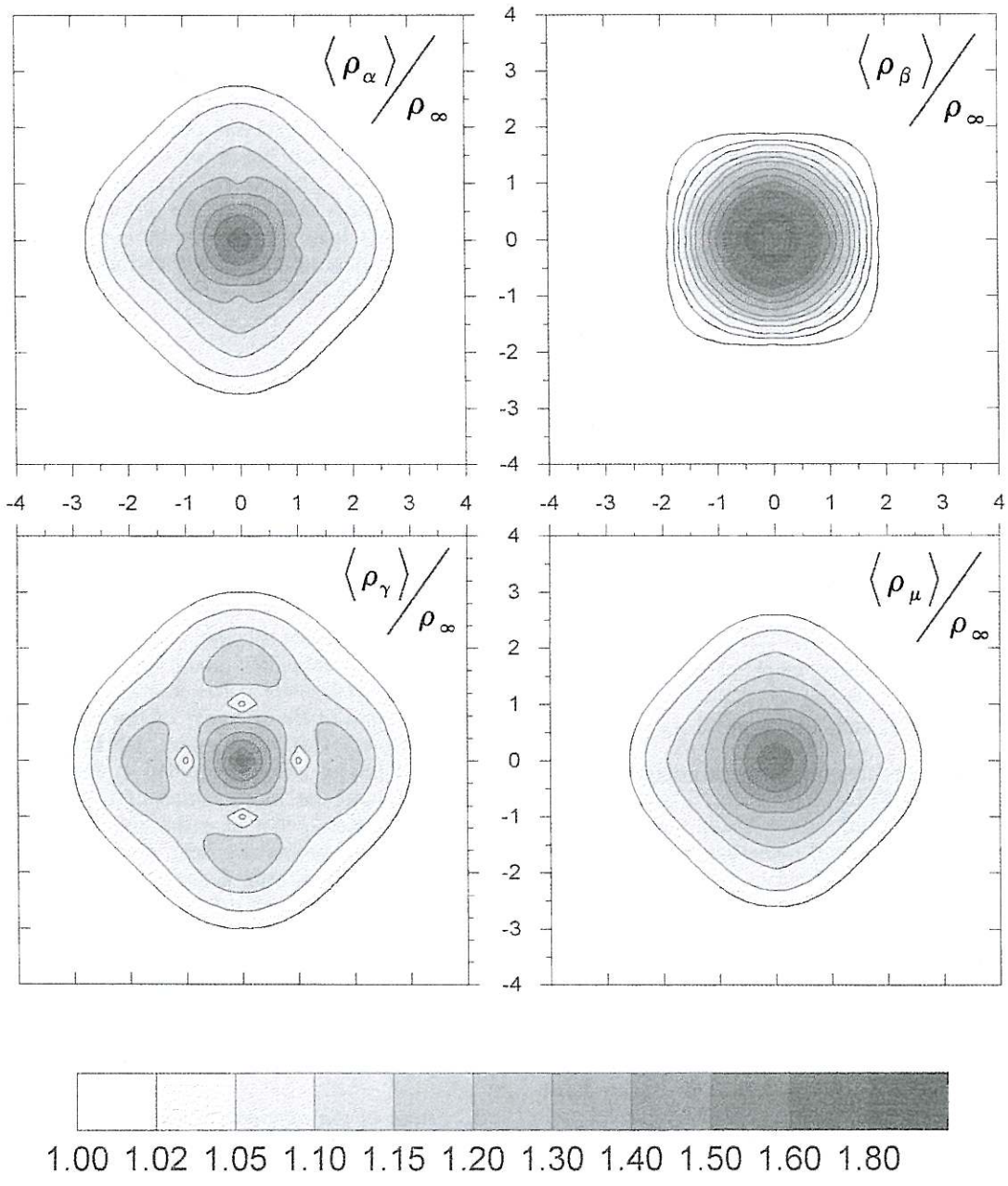

Fig. 2. Relative anomaly of the mean apparent resistivities and of $\langle \rho_\mu \rangle$ caused by a cavity with $a/L = 1$ and $h/L = 0.1$.

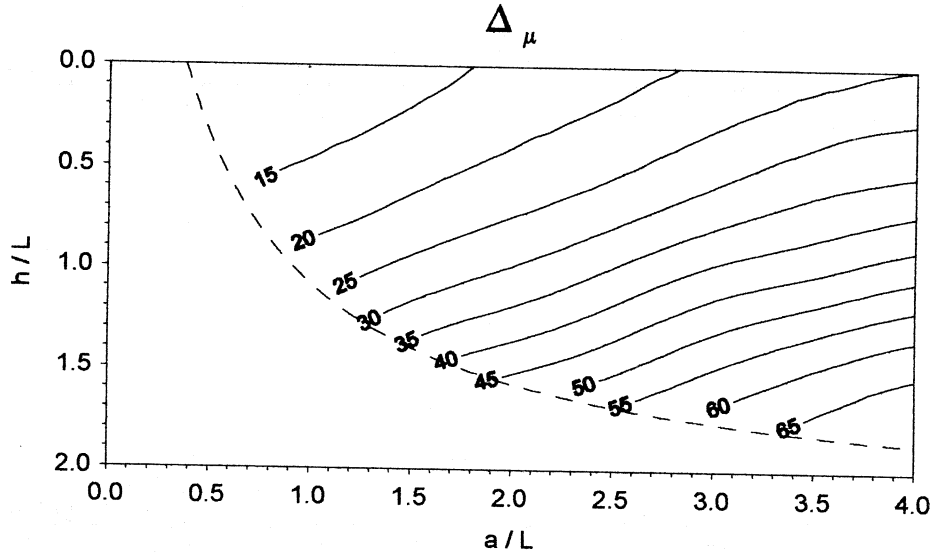

Fig. 3. Δ_μ parameter contour lines (the dashed line delimits the area of the detectable models).

problem. We will define «area of the anomaly» that area in which

$$| \psi_i | > \varepsilon \, \psi_{i\,\mathrm{MAX}}, \qquad (3.1)$$

where the real positive number $\varepsilon < 1$ is chosen on the basis of the signal/noise ratio of the measured data. The parameter ε will be $\ll 1$ when the noise level is much lower than the amplitude of the anomaly: ε will be $\cong 1$ when the noise tends to completely conceal the anomaly. The areas Δ_α and Δ_μ calculated for $\varepsilon = 0.01$ are mainly affected by the variation of the ratio h/L in the case of a cavity whose radius is smaller than the electrode spacing. The influence of the ratio a/L becomes perceptible when the depth of the sphere is greater than the electrode spacing.

Figure 3 shows the pattern of the Δ_μ contour lines in source's parameters space.

3.2. *Integral of the apparent resistivity anomaly*

Once defined the function «anomaly» of apparent resistivity as the difference between the value $\langle \rho_i(x, y) \rangle$ ($i = \alpha, \beta, \gamma, \mu, \tau$) and the background value $\langle \rho_i \rangle$ (respectively the arithmetical mean between two values perpendicularly measured in $P(x, y)$ and the mean value of the i-type apparent resistivity far from the anomalous area), we can define the relative anomaly by the equation

$$\psi_i (x, y) = \frac{\langle \rho_i (x, y) \rangle - \langle \rho_i \rangle}{\langle \rho_i \rangle} \qquad (3.2)$$

and its «volume» by the equation

$$\Psi_i = \int_A \psi_i (x_i\, y)\, dxdy, \qquad (3.3)$$

where A is the area defined in section 3.1. This parameter was calculated by a numerical algorithm, for each type of apparent resistivity and it turned out to be always strongly dependent on the geometrical parameters of the source.

The values of the volumes Ψ_α and Ψ_μ respectively for the anomalies of ρ_α and ρ_μ, show the most regular trends in the space of the models parameters and, in the case of cavity whose radius is smaller than the width of the electrodes spacing, the volume values are

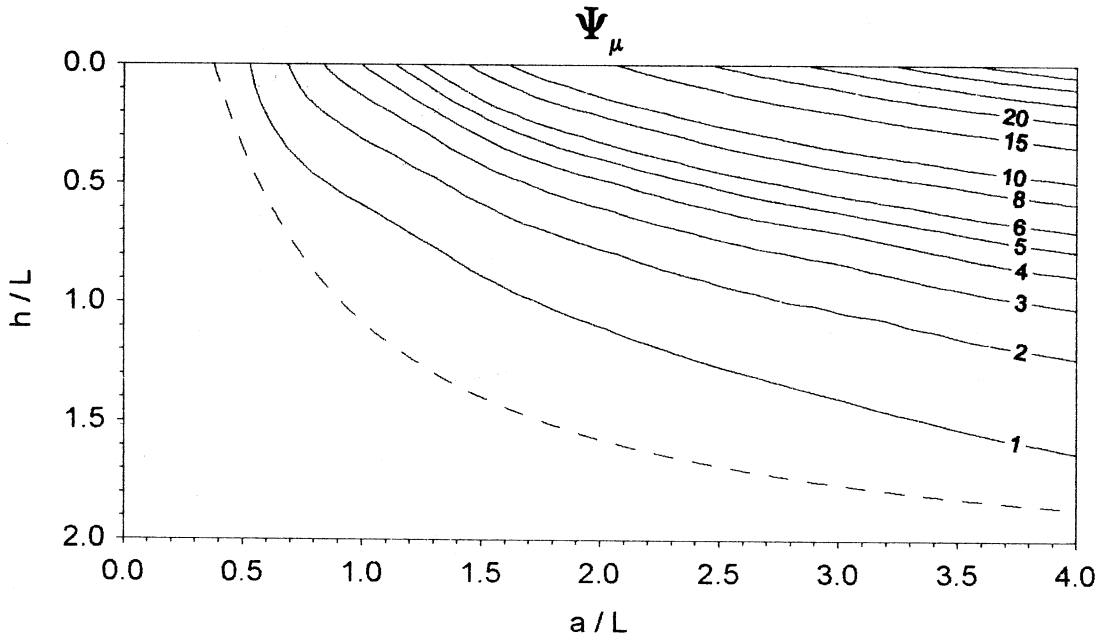

Fig. 4. Ψ_μ parameter contour lines.

strongly influenced by the ratio *a/L*, while their dependence on the ratio *h/L* becomes perceptible when the depth of the sphere is greater than the width of the array.

The dependence of Ψ_μ from the parameters of the source is shown in fig. 4.

3.3. *Parameters of azimuthal variability of the apparent resistivity*

The maps relative to the defined five apparent resistivities, measured along one of the two perpendicular directions chosen, show a marked flattening of the anomalous lines perpendicularly to the array direction. The difference between the two values, measured for each type of apparent resistivity along two perpendicular directions, generally becomes higher when the distance from the center of the anomaly increases until a limit distance after which the difference rapidly decreases. Once the two measurement directions are fixed, such difference increases when the test point moves towards one of the two profiles passing from the center of the anomaly if the distance from the center of the anomaly remains constant. The modality of this variation depends on the parameters of the source.

Then a dimensionless parameter ϑ_i is expressed for each type of apparent resistivity by the relation

$$\vartheta_i(x, y) = \frac{2\,|\rho_{i,x}(x, y) - \rho_{i,y}(x, y)|}{\rho_{i,x}(x, y) + \rho_{i,y}(x, y)}. \qquad (3.4)$$

The surface integral Θ_i of the function $\vartheta_i(x, y)$ on the whole anomaly area grows when the ratio *a/L* increases and *h/L* decreases. Because of the Θ_i contour lines regularity on the (*a/L*, *h/L*) plane this parameter can also be considered *a priori* useful to solve the inverse problem.

Figure 5 shows the pattern of the Θ_γ contour lines in source's parameters space.

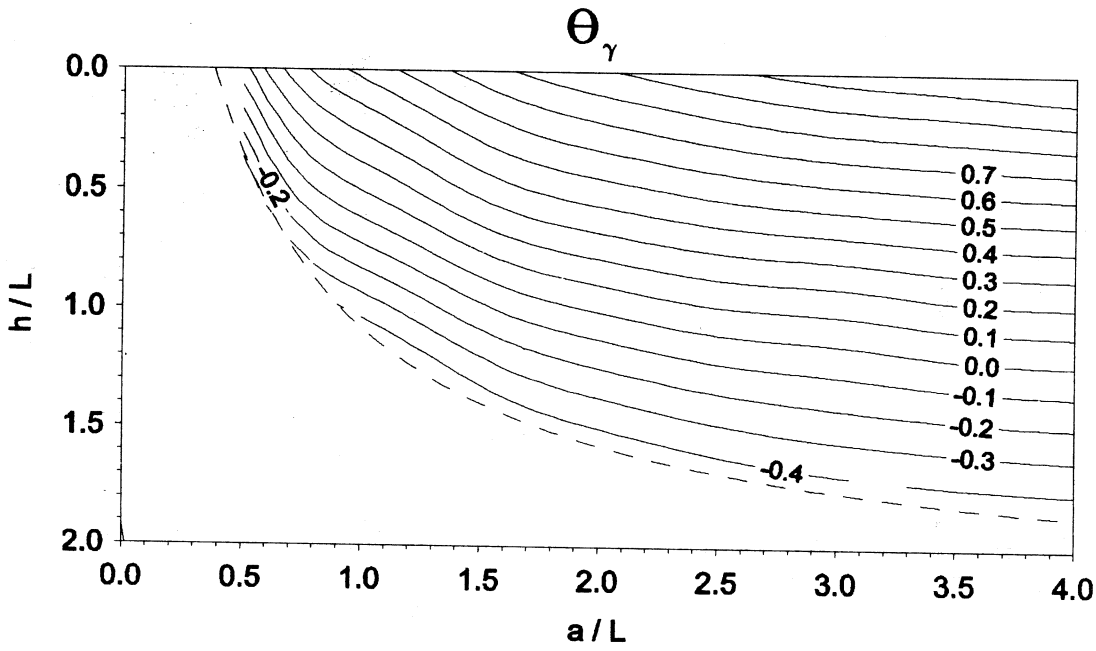

Fig. 5. Θ_γ parameter contour lines.

3.4. *Integral of the lateral variability index*

It is easy to demonstrate that among the three measures of apparent resistivity ρ_α, ρ_β and ρ_γ the last two always have extreme values; each of them assumes a minimum or maximum value when the position of the measurement point varies as to the anomalous body (Habberjam, 1969).

Acworth and Griffiths (1985) demonstrated that the ratio between two such resistivities shows the greatest variations when measured near to the main lateral changes in resistivity.

On the basis of such characteristics of ρ_β/ρ_γ and of $\rho_\beta - \rho_\gamma$ and considering that this difference tends to zero when the distance between the measurement point and the center of the anomaly increases, it seems useful to define the average parameter

$$\Lambda = \int_A \frac{\rho_\beta - \rho_\gamma}{\rho_\gamma} dxdy, \qquad (3.5)$$

where A is an area which comprises the anomaly.

The parameter Λ has a negative value for almost all the investigated models; it decreases when the cavity radius increases and generally slowly increases when the depth increases. The pattern of the contour lines Λ = const in the space of the models' parameters (fig. 6) differ from those of the already defined parameters. Then this parameter seems to be particularly useful *a priori* for the inversion of the experimental data.

3.5. *Dispersion index of the composed resistivity* ρ_τ

According to the previous arguments, the composed resistivity ρ_τ, which may be expressed as $\frac{\sqrt{42}}{3}(\rho_\gamma - \rho_\beta)$ (Cosentino and Luzio, 1994), can be considered a useful gauge of the resistivity spatial variability. The frequency

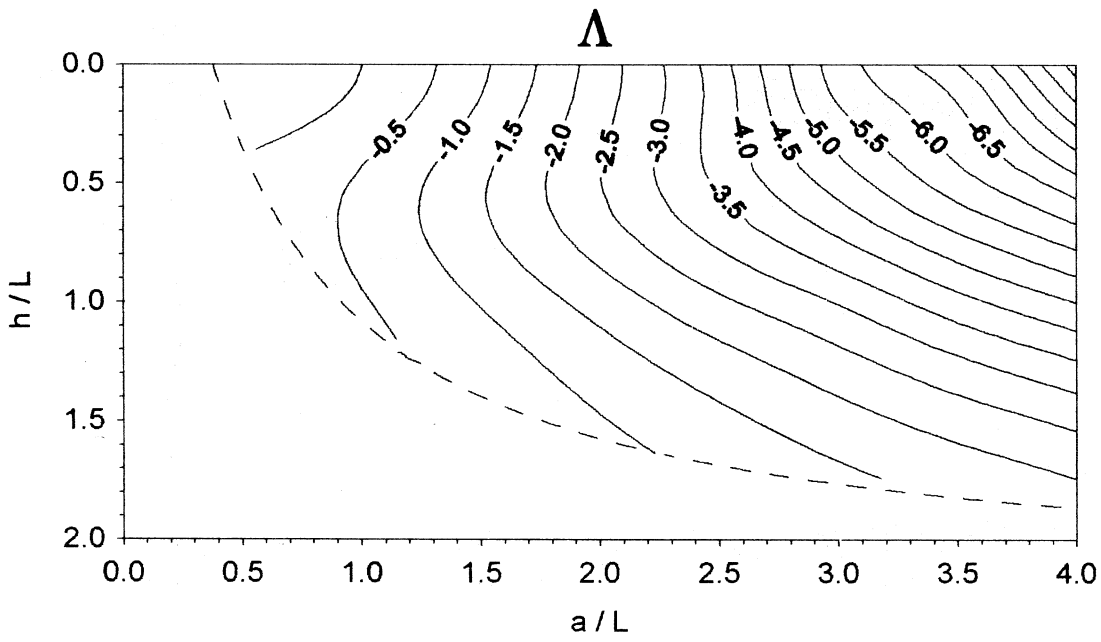

Fig. 6. Λ parameter contour lines.

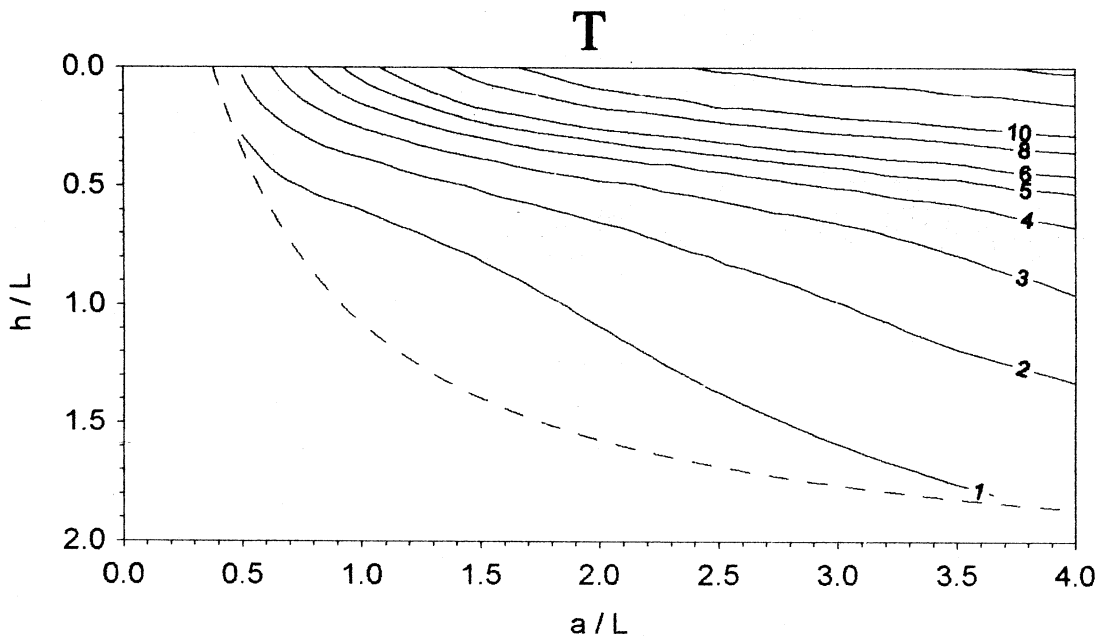

Fig. 7. T parameter contour lines.

distribution of the composed resistivities in the whole set of experimental data $f(\rho_\mu, \rho_\tau)$ generally depends on the resistivity distribution in the underground and, in the case of quasi-spherical cavities, strongly depends on the geometrical parameters of the model. A dispersion index of this distribution can be represented by the second order moment of the marginal distribution of ρ_τ.

The inversion parameter tested in this work is an estimate of ρ_τ standard marginal deviation defined as

$$T = \sqrt{\int_0^{+\infty} \int_{-\infty}^{+\infty} \rho_\tau^2 f(\rho_\mu, \rho_\tau)\, d\rho_\mu\, d\rho_\tau}\,. \qquad (3.6)$$

Figure 7 shows the T parameter contour lines in the (a/L, h/L) space.

3.6. *Some considerations*

As shown in figs. 3-7, two contour lines, relative to two different inversion parameters, intersect each other only in one point on the plane (a/L, h/L). Then there is only one spherical cavity whose tripotential response is characterized by a certain couple of values of the two parameters (with the exception of tiny portions of the space of unknown parameters and of a few couples of parameters).

The experimental estimates of the already mentioned inversion parameters will be perturbed only by measurement errors and mainly by the geological noise due to the inhomogeneity of the medium containing the cavity and the irregular shape of the latter. If the used estimators are unbiased, the real value of a parameter p_i will be included with a selected probability level in the interval

$$\bar{\bar{p}}_i - \varepsilon < p_i < \bar{\bar{p}}_i + \varepsilon \qquad (3.7)$$

where $\bar{\bar{p}}_i$ represents the parameter estimate and ε represents the width of the confidence interval.

The two inequalities (3.7) are represented by a band on the model parameters plane; the intersection of two or more bands relative to different estimated parameters, defines a region of the plane inside which each point could be the representative point of the source.

4. Inverse problem for perturbed data

In order to evaluate the characteristics of the parameter estimators and of the inversion algorithms used in the implemented procedure, the uncertainty in the estimates of the model parameters that is connected with the use of noisy data was empirically determined. For the eighty-one models analyzed the interpretation of the data was carried out by perturbing the calculated anomalies by casual increments distributed around the calculated value according to a uniform distribution with width equal to 10% of the background resistivity. This perturbation (Lowry and Shive, 1990) is, at least in non exceptional cases, an overestimate of the global effect of all the causes of non-correlated noise on the measures (measure errors, small wavelength variability in the shallow resistivity or in some physical parameters of the rocks); but it can be lower than the correlated noise due to geological bodies of dimensions comparable to or bigger than those of the investigated cavity. Figure 8a,b shows anomalies of the mean composed resistivity $\langle \rho_\mu \rangle$ for a spherical cavity model, whether in the case of perturbed data or not. For each of the eighty-one models five hundred perturbations of the spatial distributions of the ρ_α, ρ_β and ρ_γ apparent resistivities were carried out and the corresponding estimates of the nine inversion parameters (Ψ_α, Ψ_μ, Δ_α, Δ_μ, Θ_α, Θ_μ, Θ_γ, Λ, T) were calculated. The principal statistic characteristics of the sets of estimates obtained for a model characterized by a ratio $a/h = 6$ are summarized in table I. This table shows that the Ψ_i parameters have a low variance and a smaller bias than the others. On the other hand, the azimuthal variability parameters proved to be useless in the inversion because of the elevated standard deviation of the estimates and mainly because of the bias of the estimator used in this study that, as fig. 9 shows, tends to provide greatly overestimated values of the parameters.

With the punctual estimates of the six remaining inversion parameters, fifteen indepen-

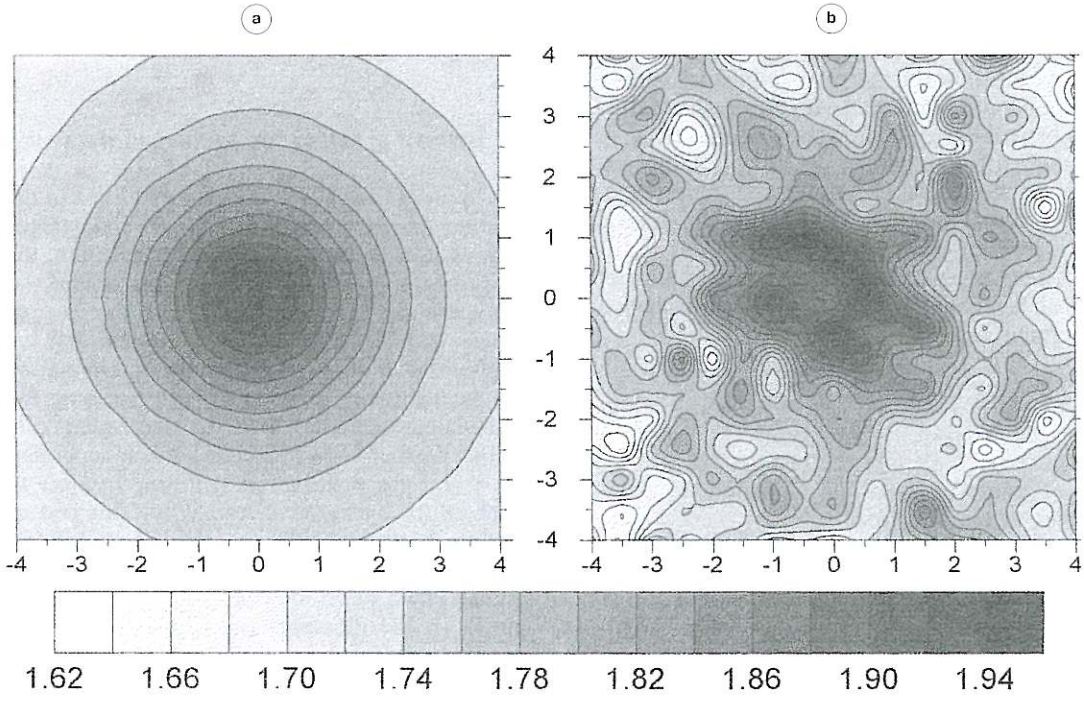

Fig. 8a,b. Mean relative anomaly of the composed resistivity ρ_μ caused by a cavity with a/L = 2.5 and h/L = 1: a) not perturbed data; b) perturbed data.

Table I. Principal statistical characteristics of the sets of the parameter estimates for a cavity model with a/L=0.5 and h/L=3.

h/L = 0.5; a/L = 3	Ψ_α	Ψ_μ	Δ_α	Δ_μ	Λ	T	Θ_α	Θ_μ	Θ_γ
Real value	7.459	6.831	34.250	28.250	−5.020	0.014	2.291	1.706	3.968
Mean	7.457	6.831	35.694	30.450	−4.933	0.015	3.661	3.206	5.649
Standard error	0.005	0.005	0.070	0.059	0.009	0.000	0.006	0.006	0.008
Standard deviation	0.109	0.106	1.566	1.322	0.202	0.000	0.134	0.127	0.187
Variance	0.012	0.011	2.452	1.749	0.041	0.000	0.018	0.016	0.035
Range	0.568	0.573	9.003	8.250	1.217	0.002	0.922	0.866	1.160
Minimum	7.172	6.554	31.500	26.750	−5.506	0.014	3.205	2.733	5.034
Maximum	7.740	7.127	40.503	35.000	−4.289	0.016	4.127	3.599	6.194
Bias	0.002	0.000	−1.444	−2.200	−0.087	−0.002	−1.370	−1.500	−1.681
Bias %	0.021	0.007	−4.217	−7.787	1.739	−13.128	−59.788	−87.941	−42.372

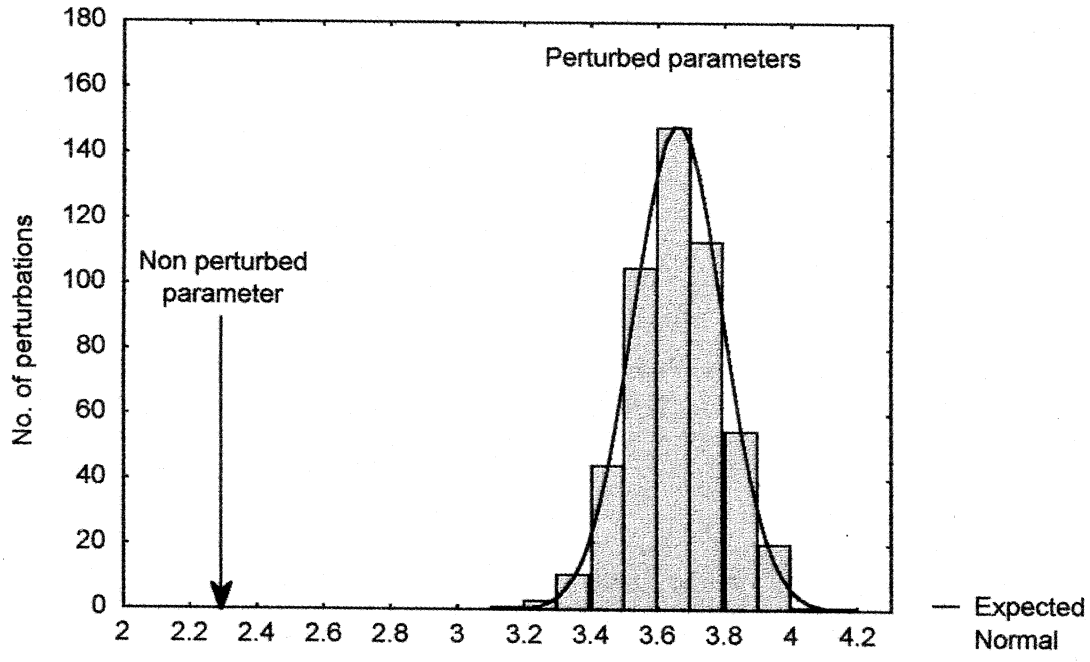

Fig. 9. Frequency histogram of the θ_μ estimates relative to five hundred perturbations of the calculated data.

dent estimates of the source parameters can be carried out for a set of experimental data. In the whole set of tests the area of the model space covered with the distribution of such estimates always contained the representative point of the source model that is not far from the average point of the whole estimates. Three of fifteen partial estimates, obtained from the couples of the inversion parameters $[\Psi_\alpha, T]$, $[\Psi_\mu, T]$, and $[\Delta_\alpha, \Delta_\mu]$ proved to be excessively unstable and distorted; this suggested their removal from the inversion procedure. Then the ultimate estimate of the model parameters can be obtained as the average point of the twelve remaining partial estimates. The distribution, in parameters space, of such estimates was sampled by means of five hundred perturbations of the calculated data, carried out as mentioned. Figure 10a,b shows an example of distribution of such estimates for two of the examined models. In particular fig. 10a shows a bias of about 5% in a/L and about 2% in h/L, low standard deviations in comparison to the bias and an evident correlation in the estimate errors of the two unknown parameters. Figure 10b shows a bias of about 4% in a/L and about 18% in h/L, with standard deviations less than 10% while the correlation between the errors is still evident. A point of model space located by a suitable weighted average of the partial estimates (with increasing weights when the variance and bias of the estimate decrease) can be considered a more reliable estimate of the unknown parameters of the investigated cavity.

For a complete knowledge of the uncertainty of the determined parameters and for the implementation of a procedure based on the calculus of the weighted average of the twelve partial estimates, the study of the pattern in the model space of the variance and bias of the estimates of each inversion parameter was carried out. The results of this investigation are shown, for one of the inversion parameters, in figs. 11 and 12.

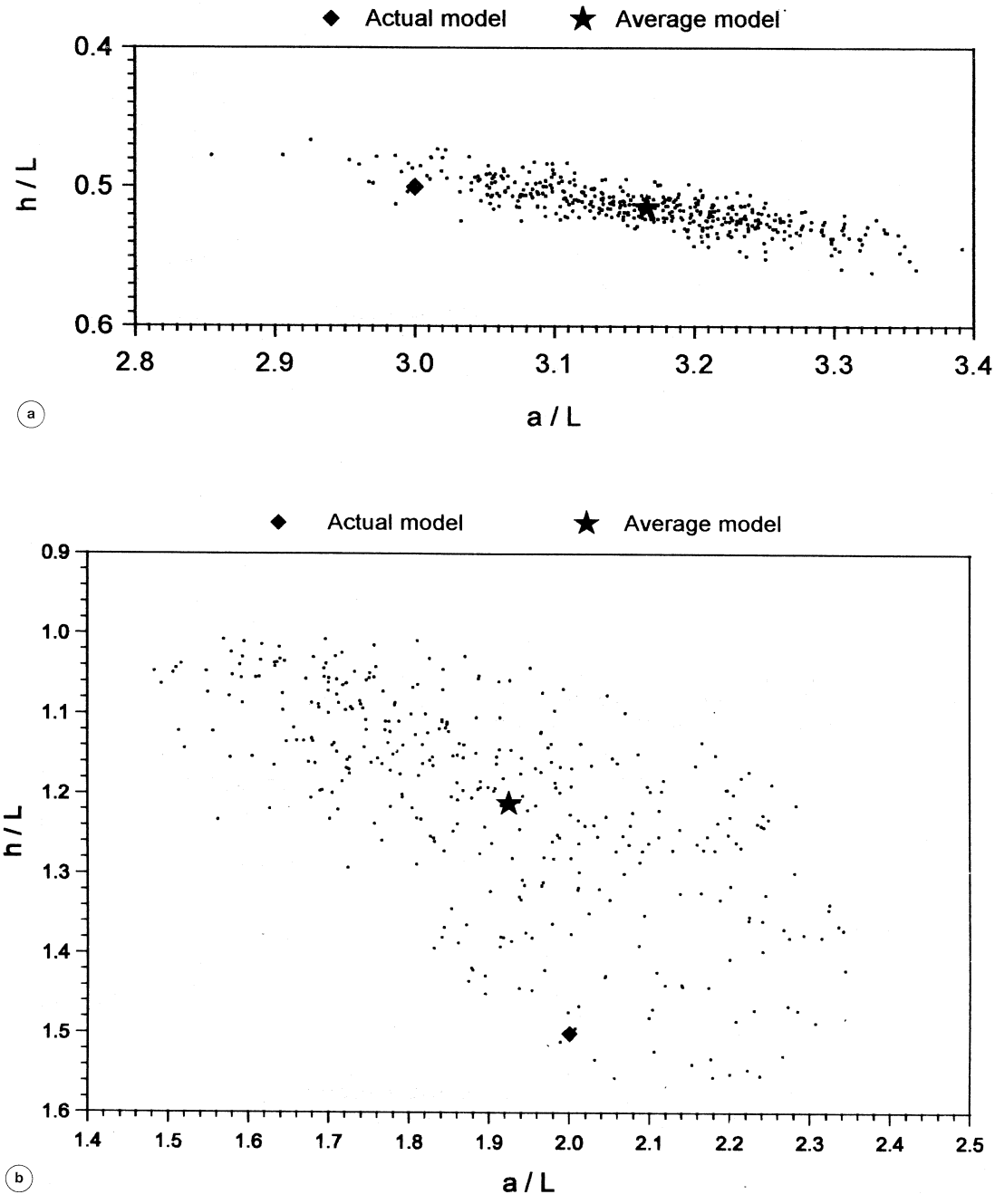

Fig. 10a,b. Distributions in the model space of five hundred estimates coming from synthetic data perturbations. Each estimate is obtained as average value of twelve partial estimates. a) Model with $h/L = 0.5$ and $a/L = 3$; b) Model with $h/L = 1.5$ and $a/L = 2$.

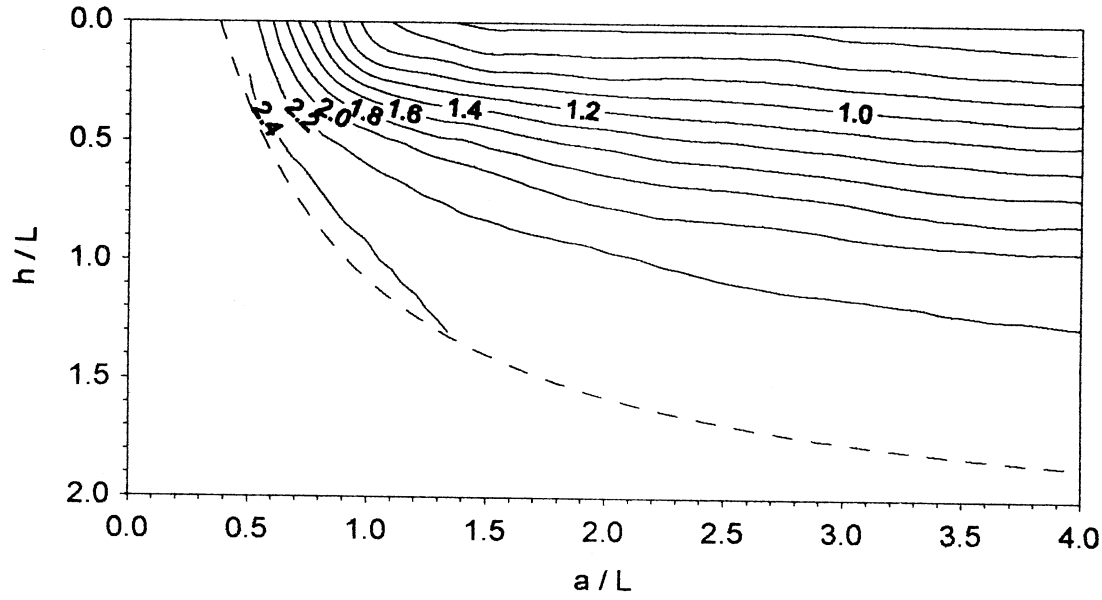

Fig. 11. Contour lines of Δ_μ parameter standard deviation.

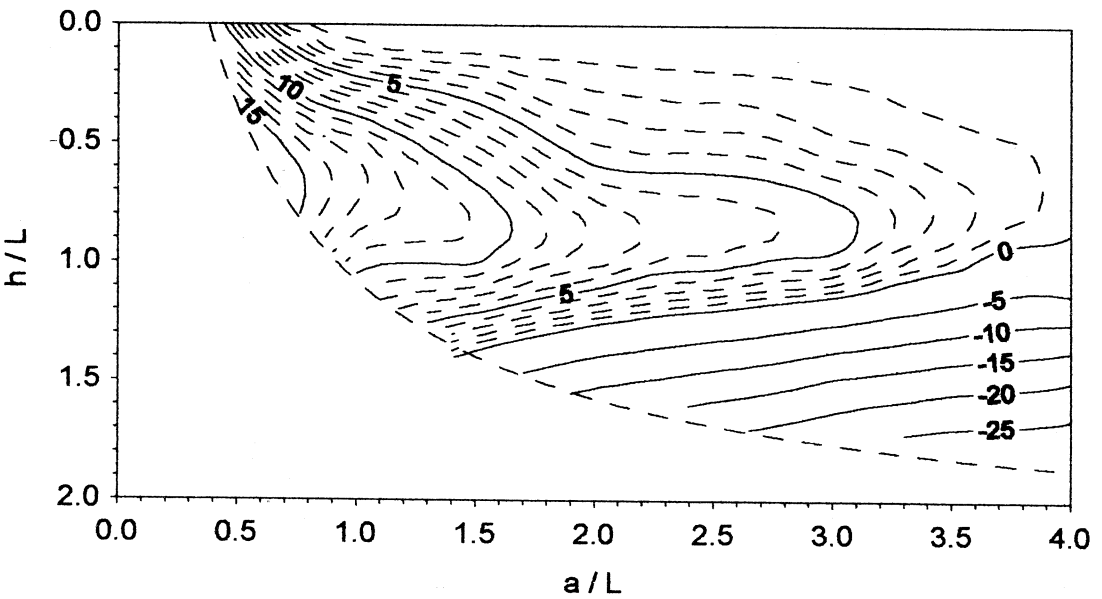

Fig. 12. Contour lines of Δ_μ parameter bias.

An inversion procedure that takes into consideration the reliability of the estimates of the inversion parameters also requires the definition and optimization of a weight function for each parameter, depending on the ratios between the variance and the bias of that parameter and those of a second one used as reference. This function generally depends on the point in model space. It should be stressed that, in order to optimize the weights assigned to the unknown parameters caused by a pair of *inversion parameters*, an iterative procedure should be used.

5. Conclusions

The statistical analysis of the parameter estimates obtained by the perturbations of the calculated data (486 values of apparent resistivity relative to eighty-one models) describes the trend of the biases and the standard deviations of the *a/L* and *h/L* estimates. Both the bias and the standard deviation as well as *a/L* and *h/L* are highly variable in model space. With reference to the portion of model space named «area of detectable models» drawn in figs. 3-7 and 11-16 we conclude that the relative bias of the *h/L* estimates (fig. 13) generally increases at the borders of such area, especially for low values of *a/L*, being less than 10% of the parameter value in a large portion of the whole area. In the band of the area $1.5 < h/L < 2$ the bias increases with *h/L* up to ~30% of the true value.

The relative bias of the *a/L* estimates (fig. 14) remains lower than 20% in the portion of the area of detectable models characterized by $h/L > 0.5$; in the thin remaining band the cavity radius is remarkably underestimated, probably because the complexity of the response produces considerable biases on the estimates of some inversion parameters and, in particular, on the anomaly area Δ_i. In order to better estimate this parameter the choice of the threshold value ε (relation (3.1)) should be optimized.

The standard deviations of *h/L* and *a/L* (figs. 15-16) are acceptable in the whole area of detectable models. While they have a minor dependence on *a/L*, that on *h/L* is instead

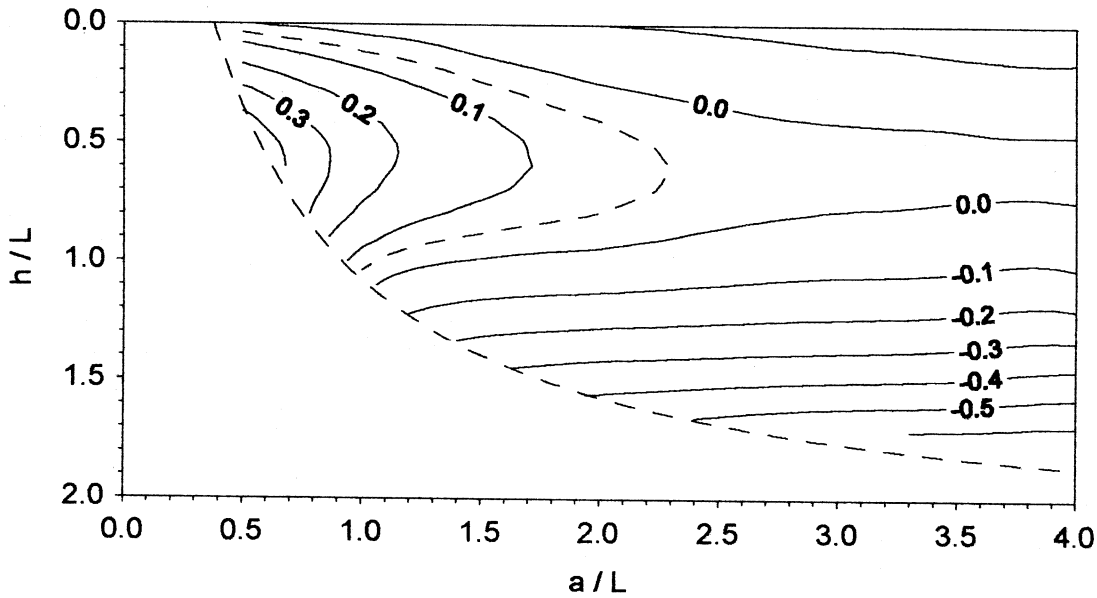

Fig. 13. Contour lines of *h/L* unknown parameter bias.

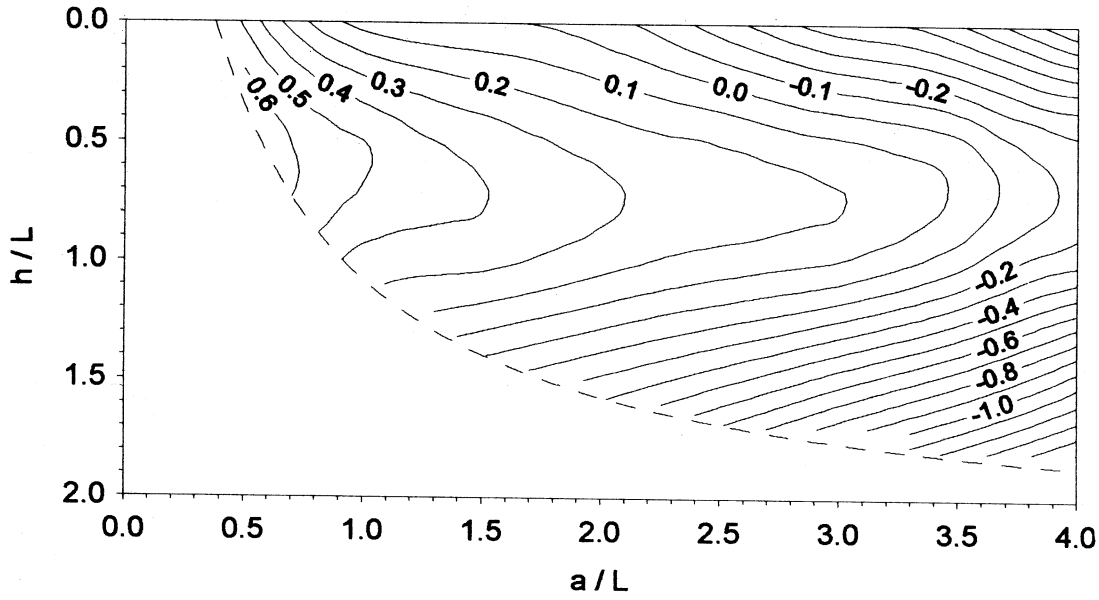

Fig. 14. Contour lines of *a/L* unknown parameter bias.

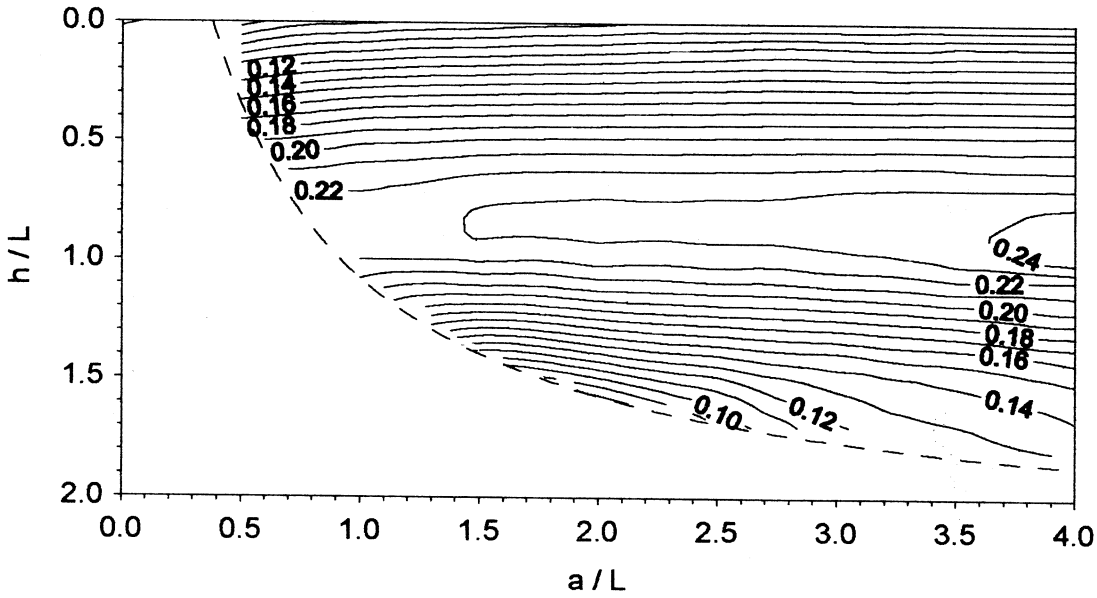

Fig. 15. Contour lines of *h/L* unknown parameter standard deviation.

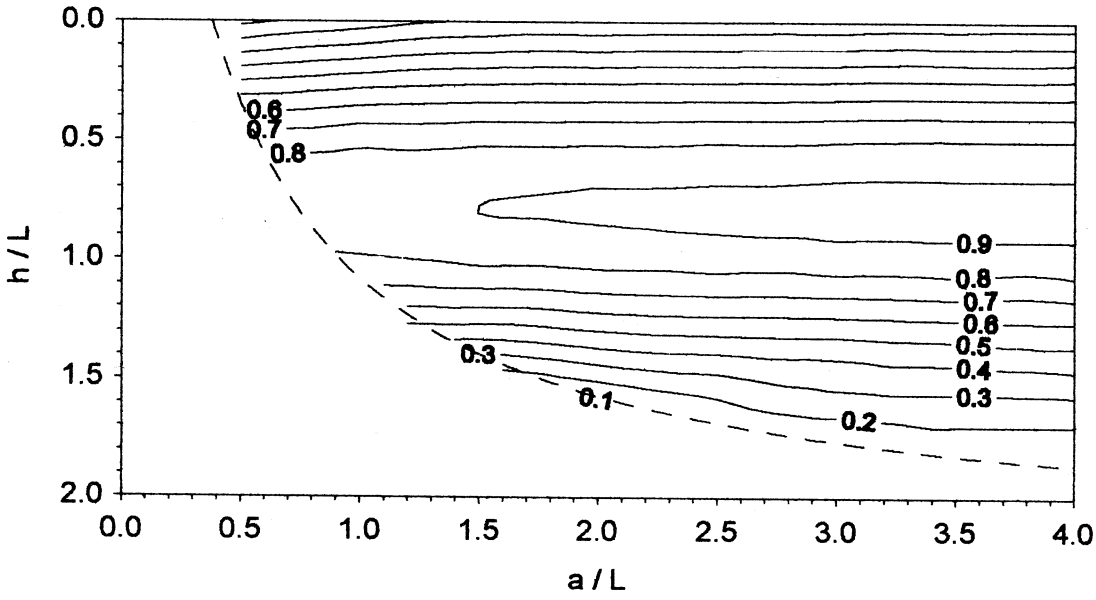

Fig. 16. Contour lines of a/L unknown parameter standard deviation.

significant, as is evident by an increase up to h/L ~0.8, to then drop off.

It is very difficult to evaluate the quality of the results that could be obtained by interpreting the data of a tripotential survey using the proposed method, mainly because no other inversion technique is readily comparable for this type of model. In fact the usual techniques for 2D and 3D interpretation of geoelectrical data are based on the approximate solution of the direct problem by various methods (for example the finite differences method) and on subsequent iterative corrections of the parameter values. These techniques, often difficult to use because of the high number of unknown parameters that must be managed, may allow a refinement of a good initial model but do not provide stable estimates of the average main parameters for the anomaly sources. On the contrary, the method here proposed, based on the computation of integral functionals of the experimental data, provides stable estimates. As a matter of fact, in our procedure any geoelectrical noise characterized by an average value smaller than the amplitude of the anomaly has small effects on the inversion.

Even if the maximum detection limit of h/a ratio is about 1.1 in the case of data with low level noise (maximum calculated anomaly is about 4% of the background resistivity), the quality of the interpretation seems susceptible of further improvement:

– if the causes of bias are identified, or

– using further inversion parameters, any of which are already argument of study, or

– assigning to each pair of parameters used for the partial inversions a weight depending on the expected standard deviation of the estimates.

The electrode areal distribution used in this work could be changed to increase the investigation depth, without reduction of the lateral resolution. The present choice aims to simplify the acquisition of the data because it allows, with a net of $n \times n$ constant spacing electrodes, to carry out quickly, by means of automatic commutations, 6 $n(n-3)$ measures of the apparent resistivities ρ_α, ρ_β and ρ_γ, of Wenner type with electrode spacing equal to the side of the mesh, 6 $n(n-5)$ measures with electrode

spacing twice the side of the mesh, and so on. Many other independent data of apparent resistivity, probably useful in the interpretation, could be still acquired by the same electrode array, if non linear and non constant spacing configurations are used.

REFERENCES

ACWORTH, R.I. and D.H. GRIFFITHS (1985): Simple data processing of tripotential apparent resistivity measurements as an aid to the interpretation of subsurface structure, *Geophys. Prospect.*, **33**, 861-887.

COSENTINO, P., and D. LUZIO (1994): Tripotential data processing for H.E.S. interpretation, *Annali di Geofisica,* **37** (suppl. 5), 1295-1302.

COSENTINO, P., E. GAGLIANO CANDELA and D. LUZIO (1992): Integrated geoelectrical investigations on the east hill in the Selinunte Archaeological Park, *Boll. Geofis. Teor. Appl.*, **34**, 181-192.

HABBERJAM, J.M. (1969): The location of spherical cavities using a tripotential resistivity technique, *Geophysics*, **34,** 780-784.

LARGE, D.B. (1971): Electric potential near a spherical body in a conducting half-space, *Geophysics*, **36**, 763-767.

LOWRY, T. and P.N. SHIVE (1990): An evaluation of Bristow's method for the detection of subsurface cavities, *Geophysics*, **55**, 514-520.